Journal of Alloys and Compounds 506 (2010) 620–625

Contents lists available at ScienceDirect

Journal of Alloys and Compounds

journal homepage: www.elsevier.com/locate/jallcom

Deformation and energy absorption characteristic of Al_2O_{3f}/Zn–Al composite foams during compression

J.A. Liu [a], S.R. Yu [a,*], Z.Q. Hu [b], Y.H. Liu [a], X.Y. Zhu [c]

[a] Key Laboratory of Automobile Materials (Jilin University), Ministry of Education, and College of Materials Science and Engineering, Jilin University, Changchun 130025, China
[b] Roll Forging Research Institute, Jilin University, Changchun 130025, China
[c] Institute of Mechanical Science and Engineering, Jilin University, Changchun 130025, China

ARTICLE INFO

Article history:
Received 10 May 2010
Received in revised form 14 June 2010
Accepted 16 June 2010
Available online 25 June 2010

Keywords:
Composite foams
Zn–Al alloy
Short fibers
Compressive behavior
Energy absorption characteristic

ABSTRACT

In this study, Zn–Al matrix composite foams reinforced with Al_2O_3 short fibers (Al_2O_{3f}/Zn–Al composite foams) were fabricated with the melt foaming process. The compressive properties and the energy absorption characteristics of the composite foams were investigated. To obtain the failure behaviour, the deformation of the composite foams was observed by scanning electron microscope (SEM). The results show that the microstructures of the foams have a significant effect on the compressive behavior of the composite foams. The strengthen mechanisms of the fiber on compressive properties of the composite foams were presented. Furthermore, the composite foams exhibit a high energy absorption characteristic.

1. Introduction

Metallic foams are considered as the structural and functional materials, which can be used to absorb impact energy during the collision. Therefore, they are adopted for protective aim in the traffic and aerospace industry [1,2].

Metallic foams can be produced by melt foaming process [1–3]. In this fabrication technique, some viscosity increasing agents such as SiC, SiO_2 and MgO particles are added into metallic melt in order to make the melt get an appropriate viscosity. Some researchers suggested that the viscosity increasing agent not only stabilized the cell wall but also affected the mechanical properties of the foams [3–7].

Generally, the mechanical properties of metallic foams depend on the relative density of the foams, the macrostructure of the cell, and the microstructure of the cell wall material [7–10]. There have been considerable researches about the effect of the cell macrostructures on the mechanical properties of the foams. However, the studies on the correlation between microstructure and compressive properties of metallic foams are scarce. Some investigations exhibited that the secondary phase or component such as viscosity increasing agent, the brittle phase and eutectic phase in cell wall material is an important factor affecting the mechanical response of the foams [9–14]. Markaki and Clyne [13] examined the mechanical properties of three closed-cell foams with similar relative densities and cell structures but evident differences in cell wall microstructure and found that cell wall ductility and toughness were impaired by high volume fractions of coarse eutectic, fine oxide films, and large brittle particles. Moreover, Yu and coworkers [9] found that the presence of SiC_p particles in ZA22–SiC_p composite foams resulted in large stress fluctuation during compression, and this led to a slightly high energy absorption capacity and a low energy absorption efficiencies as compared with ZA22 foams.

Recently, short fibers utilized as a new kind of viscosity increasing agent were proved available for the fabrication of metallic foams [15,16]. The comparison between the composite foams reinforced by short Al_2O_3 fibers and the unreinforced foams in macro-scale highlighted some advantages of fiber reinforcement [15]. However, further understandings on the deformation of foams in micro-scale are still required in order to gain the failure micro-mechanisms of the composite foams. Thereby, the compressive characteristics of Al_2O_{3f}/Zn–Al composite foams were investigated in this paper.

2. Experimental

2.1. Fabrication of the foams

The materials for preparing foams included ZA22 alloy (22.0 wt.%Al, 1.0 wt.%Cu, 0.03 wt.%Mg, and Zn balance) and Al_2O_3 short fibers. The mechanical and physical properties of the short fiber are shown in Table 1. Zn–22Al composites reinforced with 1–3 vol.% Al_2O_3 short fibers were prepared with stir-casting technique, and

* Corresponding author. Tel.: +86 431 85095862; fax: +86 431 85095876.
E-mail addresses: yusr@jlu.edu.cn, yusirong4179@163.com (S.R. Yu).

0925-8388/$ – see front matter © 2010 Elsevier B.V. All rights reserved.
doi:10.1016/j.jallcom.2010.06.107

Table 1
The mechanical and physical properties of the short fibers.

Composition		Crystal structure	Density (g/cm^3)	Strength (GPa)	Mean diameter (μm)
α-Al_2O_3 (wt.%)	SiO_2 (wt.%)				
80	20	α-Al_2O_3 Mullite	3.2	0.8–1.5	11

then it was remelted to 590 °C. Afterwards, $CaCO_3$ powders used as the blowing agent were added into the vortex of the composite melt at a stir rate of 900 rpm. Then the composite slurry was held at 700–720 °C for several minutes to allow the blowing agent to release gas bubbles. Finally, the composite foams were cooled down.

2.2. Compression tests

The dimensions of the compressive specimens were 15 mm × 15 mm × 30 mm. The compressive tests were carried out at a nominal strain rate of 2.2×10^{-3}. The obtained data were used for drawing the compressive stress–strain curves. In order to obtain the deformational micro-mechanism, the small foam samples (10 mm × 10 mm × 12 mm) were utilized. The rectangular sections of these small samples were polished, and then the samples were compressed at certain strain. Afterwards, the polished sections of the samples were observed immediately by scanning electron microscopy (Model JSM-5310, Japan) without any further metallographic treatment. The whole process is described in Fig. 1.

2.3. Characterization of the foams

The microstructures of the composite foams were observed by means of SEM. The relative density of the foams, ρ^*/ρ_s, is defined here as the ratio of the apparent density of the foams (ρ^*) to the solid density of the cell wall material (ρ_s). In this study, the mean cell size of the foams is about 2.7 mm and the pore shapes are polygonal.

3. Results and discussion

3.1. Microstructure of the composite foams

Generally, the mechanical properties of metallic foams depend on the property of cell wall material [4–7], the relative density [1–3], and the cell structure [8,9]. For Al_2O_3 short fibers reinforced Zn–22Al composite foams, the microstructure may play an important role on the compressive properties of the composite foams. Therefore, the distribution of the short fibers in the composite foams was firstly observed to try to clarify the deformation micromechanism of the composite foams.

The distribution of Al_2O_3 short fibers in the composite foams is shown in Fig. 2. It can be seen that Al_2O_3 short fibers are mainly situated on three locations in the composite foams: first, some short fibers entirely embed in the cell wall (Fig. 2(a)). This condition is similar to the distribution of the reinforcements in bulk metal matrix composites. Fig. 2(a) also indicates the random orientations of Al_2O_3 short fibers in the cell wall because the fibers are observed in both perpendicular and longitudinal orientation in the metal matrix. Secondly, according to Fig. 2(b) and (c), some short fibers partially protruded from the cell wall. This condition is somewhat different from the microstructure of short fibers reinforced bulk metal matrix composites. Thirdly, it also can be seen in Fig. 2(d) that a single short fiber penetrated through the cell. This case is evidently different from bulk metal matrix composites. In addition, it can be observed that the fibers appear to parallel to the cell wall surface in later two conditions.

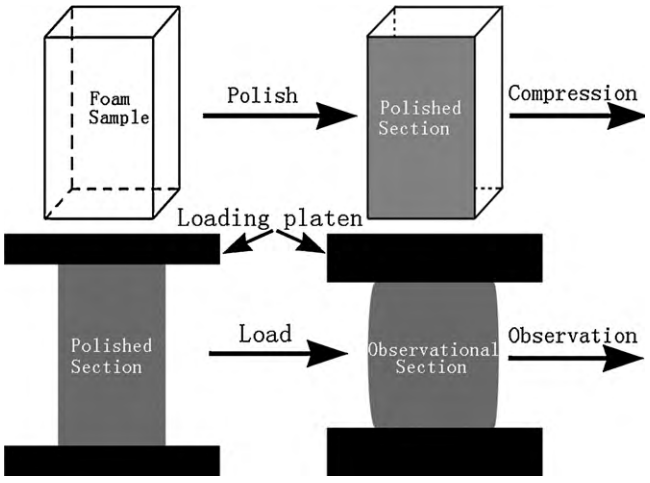

Fig. 1. Observational process of composite foams.

3.2. Compressive curves of the foams

The compressive $d\sigma/d\varepsilon$–ε curve and σ–ε curve of Al_2O_{3f}/ZA22 composite foams are shown in Fig. 3. It can be seen that the compressive σ–ε curve of the composite foams exhibits generally three regions, i.e. the elastic region, the plastic plateau region, and the densification region. Precise identifications of densification strain and yield strain are difficult for metallic foams because the stress–strain behavior of metallic foams varies with the type of foams, the component of alloy, and the fabrication process for foams [2,8,15]. The densification strain is regarded as the strain at which the slope of the tangent to the stress–strain curve tends to the elastic modulus of the matrix metal [17]. The densification strain was usually determined as the onset of the densification and taken to be the intersection of tangents to the stress–strain curve for the cell wall collapse region and densification region, as suggested by Paul and Ramamurty [18]. However, the application of this method is somewhat difficult. Thereby, for determining the yield strain and densification strain, the uniform approach was tried to establish as follows:

(1) Compressive $d\sigma/d\varepsilon$–ε curve of the composite foams is drawn based on the data obtained from the compressive experiment, as shown in Fig. 3. The stationary points ($d\sigma/d\varepsilon = 0$) in the curve were obtained.
(2) The denotation around the stationary point was checked ranging from $\varepsilon = 0$ to $\varepsilon = 0.1$. The compressive strength, σ_s, is identified as the first point around which the left denotation is positive and simultaneously the right denotation is negative. The corresponding strain, ε_s, is defined as the yield strain, i.e. the dividing line between the elastic region and the plastic plateau region.
(3) The densification strain, ε_D, is identified as the ultimate stationary point in $d\sigma/d\varepsilon$–ε curves of the foams.

The densification strain and yield strain of composite foams is listed in Table 2. The value of ε_{D1} is fixed by using the present method, and ε_{D2} is determined as suggested by Paul and Ramamurty [18]. It can be seen that the value of ε_{D1} is close to that of ε_{D2}, though there is a little difference between these parameters. The yield strains of the composite foams range from 0.022 to 0.052 and the densification strains of the composite foams are about 0.70, indicating that the composite foams keep a nearly constant low stress over a wide range of strain.

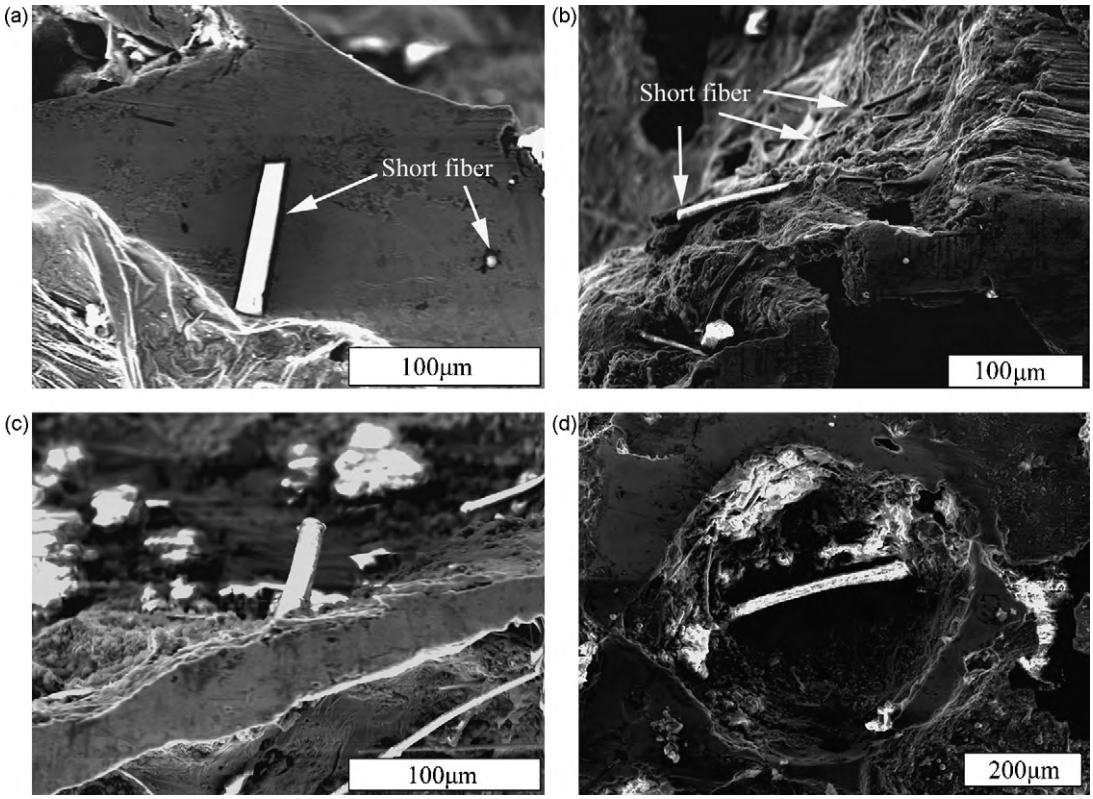

Fig. 2. Distributions of short fibers in the composite foams: Al_2O_3 short fibers (a) entirely embed in the cell wall, (b) and (c) partially protrude from the cell wall, (d) penetrate through the cells.

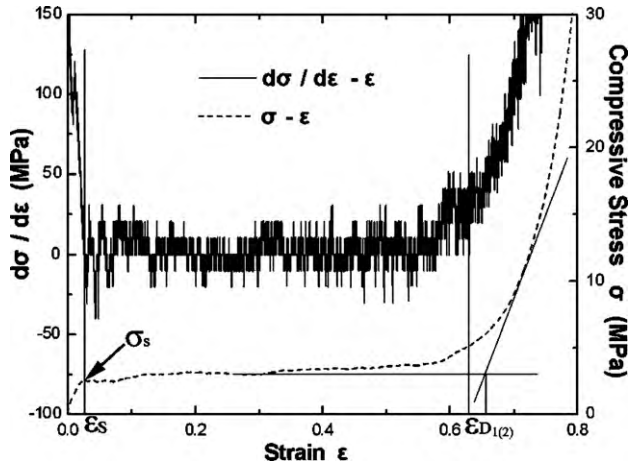

Fig. 3. Compressive $d\sigma/d\varepsilon$–ε curve and σ–ε curve of Al_2O_{3f}/ZA22 composite foams.

3.3. Failure micro-mechanisms of the composite foams

Metallic foams could fail by several mechanisms, i.e. elastic buckling, plastic yielding or brittle crushing, brittle fracture, relying on the properties of the metal matrix [17].

Table 2
The densification strain and yield strain of Al_2O_{3f}/ZA22 composite foams.

Sample	ε_s	ε_{D1}	ε_{D2}
1 vol.%Al_2O_{3f}/ZA22	0.022	0.74	0.75
3 vol.%Al_2O_{3f}/ZA22	0.023	0.65	0.68
3 vol.%Al_2O_{3f}/ZA22	0.027	0.63	0.66
3 vol.%Al_2O_{3f}/ZA22	0.052	0.68	0.70

In present study, the failure of the composite foams in macro-scale was almost controlled by the plastic yielding and a few fractures could be found which is reported in our earlier literature [15]. To understand the failure mechanism in micro-level, these fracture surfaces were observed by SEM when the composite foams failed after compression. The observations of the fracture lateral surfaces after compression revealed that the failures were primarily interfacial or matrix-dominated. Four different failure modes were obtained as follows:

First, it can be seen from Fig. 4 that the fibers were pulled out from the metal matrix and the matrix surface presented ductile dimple. There was some debris of metallic matrix on the surface of the fiber. Therefore, it can be inferred that the interface can transfer the load from the matrix to the reinforcement.

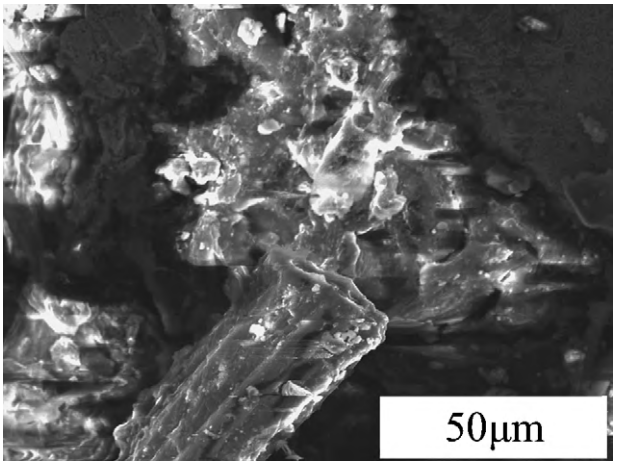

Fig. 4. Micrographs of Al_2O_{3f}/ZA22 composite foams during compression: the fiber pull-out of the matrix.

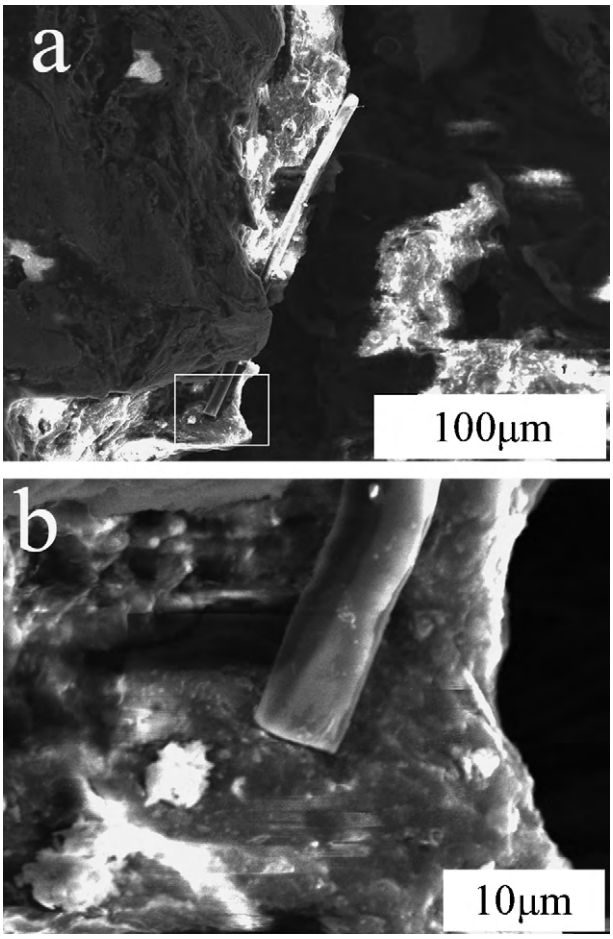

Fig. 5. Micrographs of 1 vol.% Al_2O_{3f}/ZA22 composite foams during compression: (a) a crack in a low magnification; (b) the bond of the matrix/fiber interface disengages in a higher magnification.

On contrary, a different failure mode was observed from lateral fracture surface of 1 vol.%Al_2O_{3f}/ZA22 composite foams, as shown in Fig. 5. The micrograph in a low magnification displays that the failure starts in the interface between the fiber and matrix (Fig. 5(a)). The high magnification micrograph of the crack, as shown in Fig. 5(b), suggests the surface of the fiber is smooth. That case illuminates the interface is physical combination, which provides insufficient binding force. Consequently, the poor interface results in a lower compressive strengths.

Thirdly, the failures are primarily matrix-dominated. The micrograph of Al_2O_{3f}/ZA22 composite foams during compression is shown in Fig. 6. It can be seen that the crack occurs in the matrix rather than the matrix/fiber interface. The progress directions of crack appear to suggest the fiber has a countercheck to the progress of cracks.

Fourthly, when the fiber penetrates through the cell, the strengthening effect of the fiber on the foams is different with the corresponding bulk composites. As shown in Fig. 7, the failure appears in the metal matrix without any interfacial debonding. It can be inferred that the short fiber bears the tensile and bend load, respectively. In this case, the fibers can restrict the deformation of the cell structure and reinforce the structural stability, as indicated in Fig. 8.

It can be concluded from the microstructure observations of the fracture lateral surfaces that the influencing mechanism of the fiber on compressive properties of the composite foams can be understood not only by altering the microstructure of Zn–Al matrix alloy but also by restricting the deformation of the cell structure. As

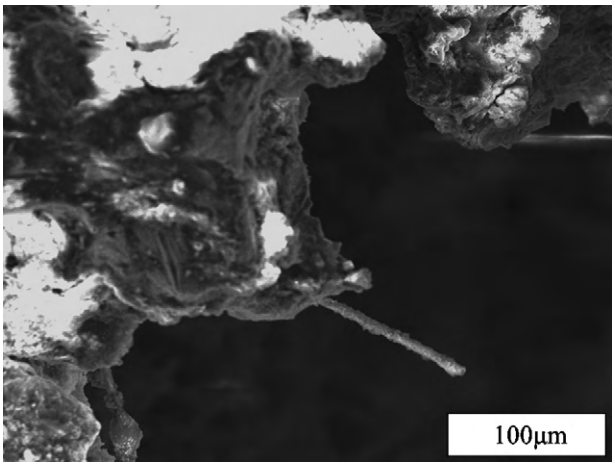

Fig. 6. Micrograph of Al_2O_{3f}/ZA22 composite foams during compression: the crack appears in matrix rather than the matrix/fiber interface.

shown in Fig. 2(a), the distribution of the short fibers is similar to that of bulk Zn–Al matrix composites. Therefore, the enhancing effects of these short fibers are similar to short fibers reinforced Zn–Al matrix composites [19,20]. Another enhancing effect can be understood from the deformation of the cell structure. As shown in Fig. 2(d), single short fiber penetrates through the cells. In this case, some cells are coupled with fiber. Increased resistance to deformation and greater structural integrity are achieved by conjunctive effect of the fiber. Whichever condition is, the interface of

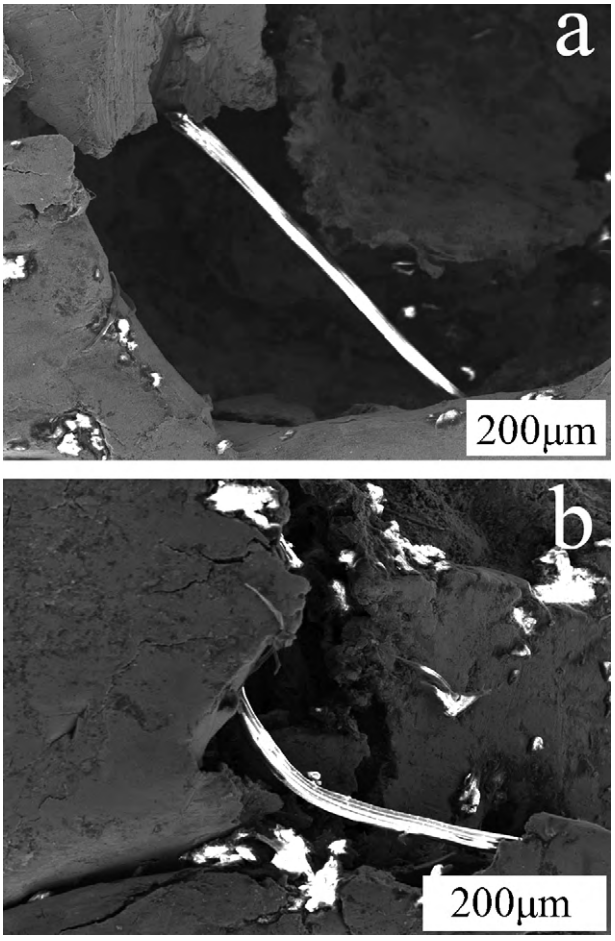

Fig. 7. Deformation and load of short fiber during compression: (a) tensile; (b) bend.

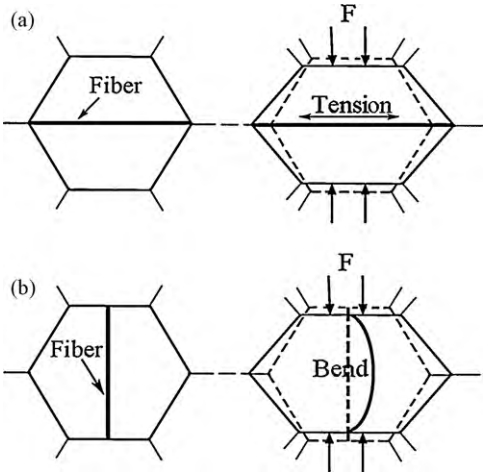

Fig. 8. Schematic diagram of the deformation and load of short fiber during compression: (a) tensile; (b) bend.

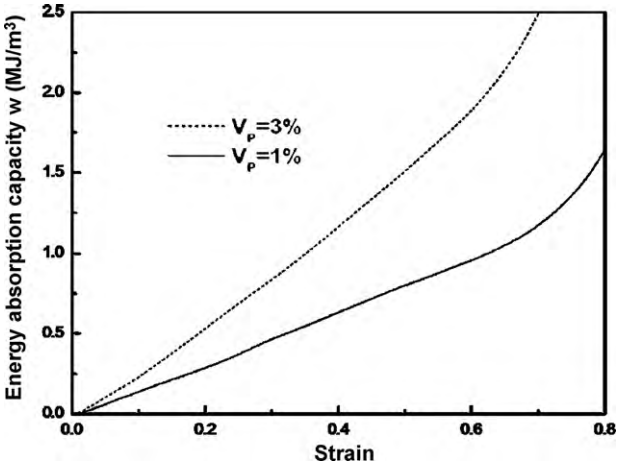

Fig. 10. Energy absorption capacities of Al_2O_{3f}/ZA22 composite foams with different volume fractions of reinforcement.

the fiber/matrix is crucial in mechanical properties of the foams. The stronger interface favors fiber-assisted localized plasticity or matrix-dominated damage whereas the weaker interface favors fiber-induced damage.

It should be noted that in this study, it is very useful that the fiber/matrix interface could be observed and expatiated quantitatively instead of speculating. Some researchers carried out the fiber pull-out test to probe the mechanical properties of fiber/matrix interface. They found that the low strength of the composite is the direct consequence of weak bonding of the interface [21,22]. Note that the illumination of the interface for the composite foams is rather difficult because of a number of irregular holes. Although the experimental results presented in this study were addressed phenomenally, further scientific signification was indicated.

3.4. Energy absorption characteristic

One of the important technological properties to estimate the application of metallic foams is energy absorption characteristic [1,2,17]. In present study, two parameters, i.e. energy absorption capacity and energy absorption efficiency were utilized to evaluate the energy absorption characteristic of the composite foams.

Energy absorption capacity of metallic foams can be obtained from the stress–strain curve [1,2], namely:

$$W = \int_0^{\varepsilon} \sigma \, d\varepsilon \tag{2}$$

where W is energy absorption capacity, ε the compressive strain, and σ the compressive stress.

Energy absorption efficiency can be calculated using the following method [23]:

$$I = \frac{\int_0^{\varepsilon} \sigma \, d\varepsilon}{\max \ \sigma|_0^{\varepsilon} \varepsilon} \tag{3}$$

where I is energy absorption efficiency, and max $\sigma|_0^{\varepsilon}$ is the maximal stress.

It is generally accepted that metallic foams can dissipate energy by the yielding, buckling, fracture of the cell structure, the friction between the cell wall fragments, and sticky flow of the gas trapped in the foams [17]. While for Al_2O_{3f}/ZA22 composite foams, the additional dissipating energy mechanism, i.e. the fiber pull-out energy and the debonding energy of fiber/matrix interface which is observed in Section 3.3, is responsible for the energy absorption.

The energy absorption capacities of Al_2O_{3f}/ZA22 composite foams are shown in Figs. 9 and 10. The energy dissipated by the composite foams during compression increases with increasing relative density. The composite foams absorb little energy in the

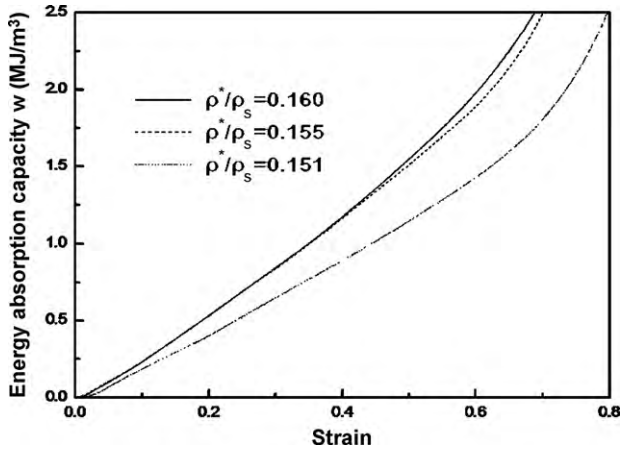

Fig. 9. Energy absorption capacities of 3 vol.%Al_2O_{3f}/ZA22 composite foams with different relative densities.

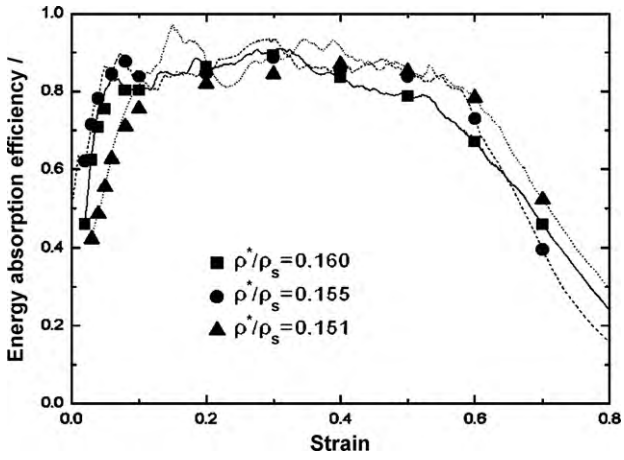

Fig. 11. Energy absorption efficiencies of 3 vol.%Al_2O_{3f}/ZA22 composite foams with different relative densities.

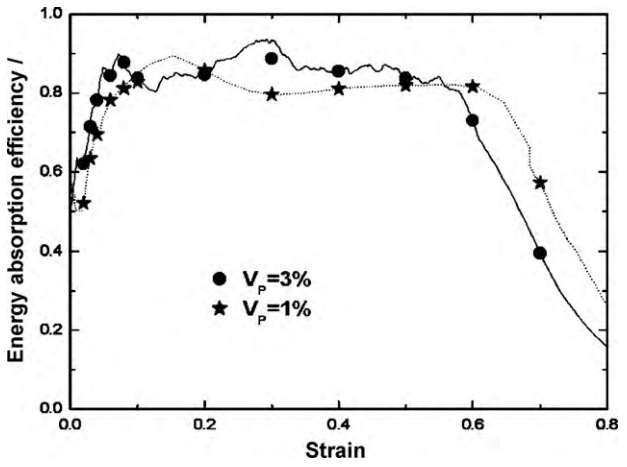

Fig. 12. Energy absorption efficiencies of Al_2O_{3f}/ZA22 composite foams with different volume fractions of reinforcement.

elastic region whereas they can dissipate much plenty of plastic deformation energy in plastic plateau region. Moreover, the foams exhibit a dependence on the volume fractions of the reinforcement. Therefore, it is drawn that the energy absorption of the composite foams derives from the resistance of metallic matrix and fiber to the compressive loads.

Energy absorption efficiencies of Al_2O_{3f}/ZA22 composite foams are shown in Figs. 11 and 12. It can be seen that the energy absorption efficiency exhibits an irrelevant tendency to relative density and the volume fractions of the reinforcement. Also, the high energy absorption efficiencies of Al_2O_{3f}/ZA22 composite foams keeping about 0.8 during the plastic plateau region indicates that the composite foams possess high energy absorption characteristic.

4. Conclusion

The deformation and energy absorption characteristic of Al_2O_{3f}/Zn–Al composite foams during compression were investigated. It is clear that, besides noticeable features like relative density, the microstructure of the foams do have a significant influence on the compressive behavior of metallic foams. There are three kinds of distributions of short fibers in the composite foams: Al_2O_3 short fibers entirely embed in the cell wall, or partially protrude from the cell wall, or penetrate through the cells. The presence of the fibers affects compressive properties of the composite foams not only by influencing the microstructure of Zn–Al matrix alloy but also by restricting the deformation of the cell structure. The strength of the fiber/matrix interface is crucial in affecting the mechanical properties of metallic foams. The energy absorption capacity of the composite foams during compression increases with increasing relative density and the content of reinforcement whereas the energy absorption efficiency exhibits irrelevant tendency to relative density and the content of reinforcement.

Acknowledgements

This work was supported by “the Fundamental Research Funds for the Central Universities (no. 421030272416)”, “Program for New Century Excellent Talents in University” and “985 project” of Jilin University of China.

References

[1] J. Banhart, Prog. Mater. Sci. 46 (2001) 559.
[2] H.P. Degischer, Handbook of Cellular Metals, WILEY-VCH-Verlag, Foreword, 2002.
[3] V. Gergely, T.W. Clyne, Adv. Eng. Mater. 2 (2000) 175.
[4] A.R. Kennedy, S. Asavavisitchai, Scripta Mater. 50 (2004) 115.
[5] S.W. Ip, Y. Wang, J.M. Toguri, Can. Met. Q. 38 (1999) 81.
[6] V. Gergely, L. Jones, T.W. Clyne, Trans. JWRI 30 (2001) 371.
[7] O. Parkash, H. Sang, J.D. Embury, Mater. Sci. Eng. A 199 (1995) 195.
[8] A.E. Simone, L.J. Gibson, Acta Mater. 46 (1998) 3109–3123.
[9] J. Liu, S. Yu, X. Zhu, et al., J. Alloys Compd. 476 (2009) 220–225.
[10] I. Jeon, T. Asahina, Acta Mater. 53 (2005) 3415–3423.
[11] S. Esmaeelzadeh, A. Simchi, D. Lehmhus, Mater. Sci. Eng. A 424 (2006) 290–299.
[12] M. Guden, S. Yuksel, J. Mater. Sci. 41 (2006) 4075–4084.
[13] A.E. Markaki, T.W. Clyne, Acta Mater. 49 (2001) 1677–1686.
[14] F. Campana, D. Pilone, Mater. Sci. Eng. A 479 (2008) 58–64.
[15] J. Liu, S. Yu, X. Zhu, et al., Mater. Lett. 62 (2008) 3636–3638.
[16] Z.K. Cao, B. Li, et al., Mater. Sci. Eng. A 486 (2008) 350–356.
[17] L.J. Gibson, M.F. Ashby, Cellular Solids: Structure and Properties, Second ed., Cambridge University Press, Oxford, 1997.
[18] A. Paul, U. Ramamurty, Mater. Sci. Eng. A 281 (2000) 1–7.
[19] S. Yu, W. Li, Z. He, J. Alloys Compd. 431 (2007) L8–L11.
[20] S. Muthukumarasamy, S. Seshan, Composites A 26 (1995) 387–393.
[21] C.Y. Yue, W.L. Cheung, J. Mater. Sci. 27 (1992) 3173–3176.
[22] J.-H. You, W. Lutz b, H. Gerger, et al., Int. J. Solids Struct. 46 (2009) 4277–4286.
[23] D. Lehmhus, J. Banhart, Mater. Sci. Eng. A 349 (2003) 98–110.